the filter effect of the product complex. It was eliminated by stepwise correction of the illumination time assuming an isosbestic point at 498 nm according to

$$t' = \sum_{m=1}^{m(\max)} (t_m - t_{m-1}) n_{m'}/n_i$$

where t' = corrected (unfiltered) illumination time, m = illumination step number, $n_{m'}$ = moles of 2 present at the extrapolated halftime between t_m and t_{m-1}, and n_i = moles of 2 initially present. Plots of n_t vs. t' gave straight lines. From their slopes the quantum yield of the zero-order decomposition of 2 was calculated.

Acknowledgment. We thank the Swiss National Science Foundation for financial support. We thank Prof. R. Scheffold (Bern) for helpful discussions and Prof. G. Calzaferri (Bern) for making his photochemical instruments available to us.

Registry No. **2**, 18195-23-8; **3a**, 107-02-8; **3b**, 78-94-4; **3c**, 107-13-1; **3d**, 126-98-7; **3e**, 140-88-5; **3f**, 97-63-2; **3g**, 79-06-1; **4a**, 123-73-9; **4b**, 497-03-0; **4c**, 930-30-3; **4d**, 930-68-7; **4e**, 623-70-1; **5a**, 107-86-8; **5b**, 141-79-7; **5c**, 638-10-8; **5d**, 4786-24-7; B_{12s}, 18534-66-2; hyroxocobalamin hydrochloride, 58288-50-9; acetic anhydride, 108-24-7.

(η^2-Olefin)(1,4-diaza-1,3-diene)dicarbonyliron Complexes. 1. Preparation and Dynamic NMR Spectroscopic Properties

Hans-Werner Frühauf,*[1a] Ingrid Pein, and Frank Seils[1b]

FB 6—Fachgebiet Organische Chemie der Universität GH Duisburg,
D-4100 Duisburg 1, Bundesrepublik Deutschland

Received October 30, 1986

The reaction of (η^4-diethyl muconate)(dad)Fe(CO) complexes (dad = 1,4-diaza-1,3-diene) with CO results in stepwise decoordination of the muconate ligand. The rates of the two consecutive displacement steps strongly depend on the properties of the respective dad ligands. Two examples of the intermediate (η^2-muconate)(dad)$Fe(CO)_2$ complexes were isolated. The complexity of their temperature-dependent NMR spectra precluded an analysis of the underlying dynamic processes. Photochemically, a series of analogous η^2-monoolefin complexes has been prepared. At low temperatures, in the rigid limiting case, their spectra are consistent with a trigonal-bipyramidal arrangement where the olefin is in equatorial position, while the dad nitrogen atoms and the two carbonyl groups occupy axial/equatorial positions, resulting in overall C_1 symmetry. A dynamic exchange process, observed in all cases, consists in rotation of the olefin about the bond to iron. With cis-disubstituted olefins, having local C_s symmetry when coordinated, simultaneous mutual exchange of the CO ligands, the dad halves, and the olefin halves is observed. This agrees with a Berry pseudorotation process, where olefin rotation occurs in the apical position of the intermediate square-pyramidal arrangement of overall C_s symmetry. The activation barriers depend (i) on the extent of π-back-bonding to the olefin, which, for a given olefin, is reduced when the more π-acidic dad ligands compete for the electron density at iron, and (ii) on the steric bulk of dad and olefin ligands. In cases where the olefin and the (dad)$Fe(CO)_2$ fragments have no symmetry element in common, a second exchange process at higher temperatures is observed which again equilibrates the two inequivalent halves of the dad ligand. This exchange cannot be effected by the former mechanism. Of the possible explanations being discussed for this second dynamic exchange process, a reversible dissociation of the olefin is strongly favored.

Introduction

Our continuing interest in the preparation, structural elucidation, investigation of spectroscopic properties, and reactivity patterns of (1,4-diaza-1,3-diene)carbonyliron complexes with organic π-ligands originates in their close relation to known active species in dad–Fe systems[2] that homogeneously catalyze the dimerization or oligomerization of unsaturated organic molecules. In the square-pyramidal coordination geometry of (η^4-1,3-diene)(dad)carbonyliron complexes **1**,[3] we have observed an interesting dependence of ligand arrangement on the π-acidity of the diene ligand. With diethyl muconate, a pronounced π-accepting diene, the two nitrogen atoms of all types of dad ligands (cf. Chart I) are coordinated in basal/apical positions, reducing the symmetry of the complex to C_1. Complexes with dienes without electron-withdrawing substituents exhibit C_s symmetry, due to N,N′ basal/basal coordination of the respective dad ligands. The latter complexes **1**-C_s are unreactive with respect to ligand substitution reactions, while the complexes **1**-C_1, with diethyl muconate, show strongly increasing substitutional lability with increasing acceptor properties of the dad ligands, e.g.,

Chart I

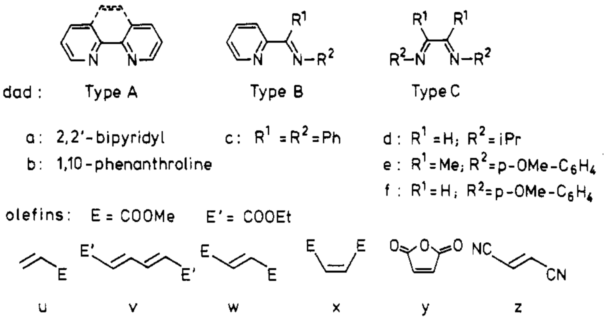

---

[1] (a) New address: Laboratorium voor Anorganische Chemie, University of Amsterdam, J.H. van't Hoff Instituut, Nieuwe Achtergracht 166, 1018 WV Amsterdam, The Netherlands. (b) Present address: Department of Chemistry, The University of Alberta, Edmonton, Alberta, Canada T6G 2G2.

[2] (a) Yamamoto, A.; Morifuji, K.; Ikeda, S.; Saito, T.; Uchida, Y.; Misono, A. *J. Am. Chem. Soc.* **1965**, *87*, 4652. (b) *Ibid.* **1968**, *90*, 1878. (c) Misono, A.; Uchida, Y.; Hidai, M. *Bull. Soc. Chem. Jpn.* **1966**, *39*, 2425. (d) Wu, Ch.-Y.; Swift, H. E. *J. Catal.* **1972**, *24*, 510. (e) Maly, N. A.; Menapace, H. R.; Benner, G. S.; Hillegas, D. V. *ACS Symposium on New Routes to Olefins*; Boston, April 1973; Abstr. No. B95. (f) tom Dieck, H.; Bruder, H. *J. Chem. Soc., Chem. Commun.* **1977**, 24.

[3] Frühauf, H.-W.; Wolmershäuser, G. *Chem. Ber.* **1982**, *115*, 1070.

in going from dad-type A to C.[3] Thus, in the presence of CO, the photochemical formation of 1-C_1 from (dad)Fe-$(CO)_3$ (**3**) is thermally reversed according to eq 1. The intermediate (η^2-muconate)(dad)Fe$(CO)_2$ complexes **2** are isolable under favorable conditions, and two examples are reported.

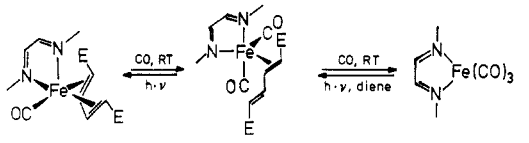

(1)

1-C_1 2 3

Ligand displacement is the essential final step in any catalytic cycle, liberating product, and, assuming a dissociative S_N1-like mechanism, creating a coordinatively unsaturated species that eventually binds to educt again to start a new catalytic cycle. From the observed strong influence of the electronic properties of the dad ligand on the rates in eq 1,[3] it was desirable to study a series of η^2-monoolefin complexes, **2**, in order to learn about the influence of both dad and π ligands on the stability of the metal–olefin bond. Further, complexes **2** are stereochemically nonrigid. The temperature-dependent NMR spectra of the η^2-diene complexes proved too complicated to be successfully analyzed. We expected that from the simpler spectra of η^2-monoolefin complexes it should be possible to extract information about the nature of the dynamic processes involved.

Here we report on the synthesis and dynamic behavior of these complexes **2**. They include one series with constant diazadiene (dad = 2,2′-bipyridyl) and variable olefin ligand and one series keeping the olefin constant (dimethyl fumarate) while varying the π-acidity of the dad ligand. In a forthcoming paper[4] we will report on what bearing these changes in electronic properties have on the stability of the metal–olefin bond.

Results and Discussion

The ligands employed in this investigation are shown in Chart I. Letters from the beginning of the alphabet identify the diazadienes of type A through C, while the olefins are given letters from the end of the alphabet.

Formation and Properties of (η^2-1,3-diene)(dad)Fe-$(CO)_2$. The η^2-muconate complexes, e.g., **2av** and **2ev**, are best prepared via the η^4-complexes **1**, i.e., by first following the photochemical reaction sequence in eq 1 all the way from right to left and then by going back one step thermally through displacement of one coordinated π-bond in the η^4-complexes. The reason is that the photochemical step **2** → **1** (cf. eq 1) is very efficient,[3] and only with the best π-accepting diazadienes the thermal reverse reaction **1** → **2** is fast enough to be competitive.

The consecutive reactions **1** → **2** → **3** are accompanied by changes in color, which in some cases allow the identification of the main constituent by visual inspection. From test tube reactions it appeared that the first step was faster than the second and that the absolute rates and perhaps also the ratio of the rates of steps one and two depended on the nature of the respective diazadiene.

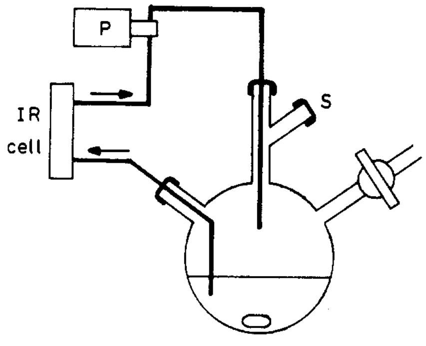

Figure 1. Scheme of the flow-cell apparatus used to IR monitor the consecutive diene displacement steps in eq 1.

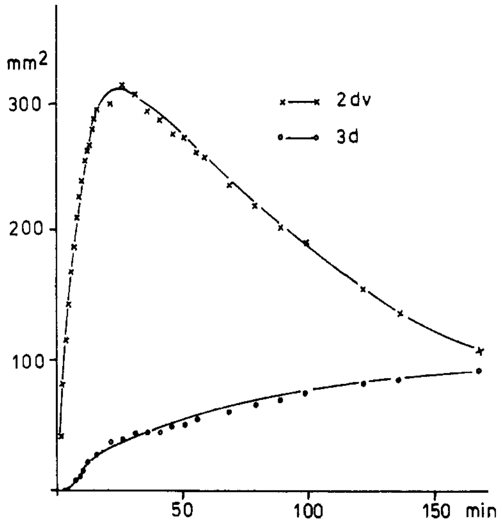

Figure 2. Consecutive reactions **1dv** → **2dv** → **3d**: shown are the areas (mm^2) of carbonyl stretching bands in the extinction mode of **2dv** (1989.3 cm^{-1}) and **3d** (2019.6 cm^{-1}) as a function of time. The disappearance of **1dv** could not be monitored as its band (1937.7 cm^{-1}) overlaps with those of **2dv** and **3d** at 1938.2 and 1942.3 cm^{-1}, respectively.

1av was the first example of a (η^4-1,3-diene)(dad)Fe(CO) complex that had been prepared.[5] Its reaction with CO in benzene solution was so slow that it could be monitored by NMR, with drawing samples at various times and quenching the reaction by degassing.[6,7] These experiments revealed that the reaction consisted in a stepwise decoordination of the η^4-muconate ligand and that the intermediate η^2-complex showed a very complicated temperature-dependent NMR spectrum. The analogous reactions with CO of muconate complexes of other diazadienes were too fast to be followed this way. To evaluate methods for a possible isolation of one or the other of the intermediate η^2-complexes **2**, it was necessary to get at least a qualitative knowledge of the rates. We therefore devised the setup outlined in Figure 1 to monitor the reaction with CO by IR in a flow cell. The apparatus was filled and flushed with CO, and then, through septum S, 20 mL of benzene solutions ca. 0.015 M in complexes **1** was injected. Circulation through the IR cell was achieved by an FMI pump, P, and the minimal time required from injection to completion of the first scan through the relevant carbonyl region was ca. 2.5 min. In the case of **1dv**, the two consecutive reactions could be clearly distinguished (cf. Figure 2), the maximum concentration of **2dv** being reached after 25 min, while **3d** began to show up after 8 min already. Obviously, the two steps have comparable rates in this case, and pure **2dv** could not be isolated. With

---

(4) Frühauf, H.-W.; Seils, F., to be submitted for publication.

(5) DePaoli, M. A.; Frühauf, H.-W.; Grevels, F.-W.; Koerner von Gustorf, E. A.; Riemer, W.; Krüger, C. *J. Organomet. Chem.* **1977**, *136*, 219.

(6) Frühauf, H.-W., Habilitationsschrift, Universität GH Duisburg, 1980.

(7) With the bipyridyl complexes, IR monitoring had not been possible because the CO stretching bands of the respective complexes **1av**, **2av**, and **3a** are broad and overlapping one another, filling the region between 2000 and 1900 cm^{-1} rather evenly.

1ev, the first step in the reaction sequence turned out to be much too fast to be observed with the given setup. When the solution had reached the IR cell, the starting complex had already completely disappeared. The second step was very slow, with roughly 10% **3e** being formed after 3 h. Thus, in this case with $k_1 \gg k_2$, **2ev** could be easily isolated. Its ^{1}H NMR spectrum, however, is even more complicated than that of **2av**, precluding an analysis of the temperature-dependent processes.

Preparation of Monoolefin Complexes 2. The collection of olefins in Chart I already indicates that to produce isolable complexes of type 2 the π-ligand is required to have at least one electron-withdrawing substituent. In principle, all complexes 2 are accessible by the photosubstitution reaction given in eq 2. However, there are several complications that need to be commented on. The most stable complexes 2 are those with a good balance between dad donor character and π-acidity of the olefin. This results in polar compounds with a spatially directed shift of electron density from the dad across the central iron into the energetically low-lying π^*-acceptor orbital of the olefin. Complexes are labilized, if this intramolecular push–pull or dipolar stabilization is prevented, i.e., if the π-acidity of the olefin is reduced and, even more so, if a diazadiene of good acceptor properties, e.g., **f**, competes for the electron density at the iron. Our findings are (vide infra) that under these conditions the olefin dissociates in solution, and, in the absence of stabilizing ligands like CO, the coordinatively unsaturated fragment falls apart; the two CO ligands thus liberated may then intercept two other (dad)Fe(CO)$_2$ fragments, the net result being partial decomposition and regeneration of tricarbonyl 3.

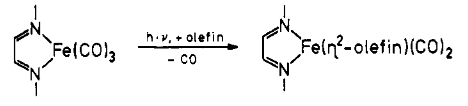

(2)

3a–f

2

au, av, aw, ax, ay, az, bw, cw, dw, ev, ew, fw

Thus, with methyl acrylate all complexes 2 are labile, and they are therefore prepared somewhat below room temperature with an excess of olefin and with purging the solution with argon to remove the CO evolved. An excess of olefin creates no problems. In no case more than one monoolefin was photosubstituted for CO in 3 to (inadvertently) generate a bis(olefin) complex. This contrasts the situation in the case of the η^2-1,3-dienes[8] where the entropy effect and the advantages of η^4-coordination make the second CO substitution very efficient.

Photochemical preparation of complexes 2 with the most π-acidic olefins like maleic anhydride (**y**) or fumaronitrile (**z**), e.g., **2ay** and **2az**, turned out to be very difficult. At room temperature, competing thermal reactions of the olefins with the tricarbonyliron complexes 3 lead to a variety of yet unidentified products.[9] Once they are formed, **2ay** and **2az** are stable at room temperature, but their high polarity creates problems. The low solubility in most organic solvents leads to precipitation on the immersion well during photolysis. Purification by recrystallization is difficult, especially since at elevated temperatures there is decomposition, presumably caused by intramolecular redox reactions. Thus, only in the case of **2az** could a pure sample be obtained this way and only in rather poor yield. Here, the dissociative process, first discovered in the η^2-muconate complexes and, in the course of this investigation, confirmed for the less π-acidic monoolefins, could be used very profitably for a thermal olefin exchange reaction. Almost quantitative yields of **2ay** and **2az** could be obtained this way from exchange of the acrylate ligand in **2au**.

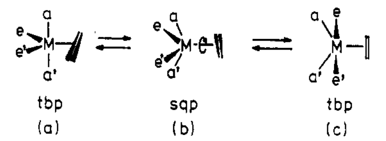

Figure 3. Schematic representation of olefin rotation coupled to Berry pseudorotation (after ref 11).

Molecular Dynamics and NMR Spectra of Complexes 2. All complexes 2 included in this investigation show temperature-dependent NMR spectra due to intramolecular exchange processes.

Olefins may be bound rigidly to a metal in a specific orientation, or they may rotate around the bond axis to the central metal atom. Calculated activation barriers for pure olefin rotation in an otherwise rigid trigonal-bipyramidal (tbp) complex[11] exceeded the normally observed experimental values[12] of 40–70 kJ/mol by a factor of 2–3. This gap vanishes, if one assumes a mechanism in which the olefin rotation occurs in the apical position of an intermediate square-pyramidal (sqp) geometry, reached by distortion during a Berry pseudorotation,[11] i.e., formula **b** in Figure 3. According to this view, e.g., in (olefin)Fe(CO)$_4$, a single rate constant would exist for olefin rotation and the eqilibration of CO ligands in axial and equatorial positions, which indeed is found in most cases. However, there are examples that are at variance with this model by showing more than one rate constant.[13,14] Also, in the case of diene–iron complexes another mechanistic explanation was favored;[15] it assumed a joint rotation of three ligands around a fixed L$_2$Fe unit. In view of these various models the NMR spectra of complexes 2 had to be analyzed very carefully. Besides potential olefin rotation, there is the chelating dad ligand coordinated to iron that may have its own, independent dynamics.

In the rigid limiting case, when exchange processes are slow on the NMR time scale, all complexes 2 in their ^{1}H NMR spectra show double sets of signals for both the olefin and dad ligands. This is in agreement with structure **a** as shown in Figure 3, where, e.g., positions e and a are occupied by the dad nitrogen atoms and e′ and a′ are occupied by the carbonyl ligands. The olefinic protons show an upfield coordination shift of 2.6–4.8 ppm, as would be expected from the increase in electron density due to π-back-bonding. Conversely, the dad protons in the immediate neighborhood of the n-donating nitrogen atoms

---

[8] Frühauf, H.-W.; Grevels, F.-W.; Landers, A. *J. Organomet. Chem.* **1979**, *178*, 349.

[9] Further investigations will show if these reactions may be comparable to those of compounds 3 with electron-deficient alkynes,[10] the initial step of which we interpret as a 1,3-dipolar cycloaddition of the alkyne to the C=N—Fe unit in 3.

[10] Seils, F. Dissertation, Universität GH Duisburg, 1986. For the most recent paper on mechanistic details of this reaction: cf. Frühauf, H.-W.; Seils, F. *J. Organomet. Chem.* **1986**, *302*, 59.

[11] Albright, T. A.; Hoffmann, R.; Thibeault, J. C.; Thorn, D. L. *J. Am. Chem. Soc.* **1979**, *101*, 3801.

[12] (a) Wilson, S. T.; Coville, N. J.; Shapley, J. R.; Osborn, J. A. *J. Am. Chem. Soc.* **1974**, *96*, 4038. (b) Kruczynski, L.; Martin, J. L.; Takats, J. *J. Organomet. Chem.* **1974**, *80*, C9. (c) Kruczynski, L.; LiShingMan, L. K. K.; Takats, J. *J. Am. Chem. Soc.* **1974**, *96*, 4006.

[13] Faller, J. W. *Adv. Organomet. Chem.* **1977**, *16*, 211 and references cited therein.

[14] Cosandey, M.; von Büren, M.; Hansen, H.-J. *Helv. Chim. Acta* **1983**, *66*, 1.

[15] (a) Kreiter, C. G.; Lang, M. *J. Organomet. Chem.* **1973**, *55*, C27. (b) Kreiter, C. G.; Stueber, S.; Wackerls, L. *J. Organomet. Chem.* **1974**, *66*, C49. (c) Kruczynski, L.; Takats, J. *J. Am. Chem. Soc.* **1974**, *96*, 932. (d) Kruczynski, L.; Takats, J. *Inorg. Chem.* **1976**, *15*, 3140.

Table I. ^{1}H NMR Data of 2: Chemical Shifts and Coupling Constants of the Olefinic Protons in the Limit of Slow Exchange

complex	solv^a	*T*, K	δ	^3J(H,H), Hz
2au	A	203	*b*	*b*
2ax	B	253	3.00/1.55	9.1
2aw	A	223	3.67/3.09	9.8
2ay	B	253	3.76/2.67	3.8
2az	B	293	2.73/2.27	9.1
2cw	A	223	3.97/3.30	9.2
2dw	A	223	4.05/3.13	9.9
2ew	A	223	4.15/3.11	10.5
2fw	A	213	4.18/2.96	10.6

^{a} A, acetone-d_6; B, acetonitrile-d_3. ^{b} Assignment uncertain due to partial overlap.

Table II. Temperatures of Coalescence and Calculated Energies of Activation from ^{1}H DNMR Spectra of Complexes 2

complex	T_c(dad),^{a} K	$\Delta G_c^{\ddagger}$(dad),^{a} kJ/mol	T_c(ol),^{b} K	$\Delta G_c^{\ddagger}$(ol),^{b} kJ/mol
2au	241	48.4 (±0.6)		
2ax	291	61.5 (±0.6)	299	60.9 (±0.6)
2aw	>313	>67	288	59.1 (±1.1)
2ay	299	62.4 (±1.1)	303	61.0 (±0.6)
2az			358	74.7 (±1.7)
2dw	≥310	≥66	263	52.9 (±1.1)
2ew			271	58.5 (±0.6)
2fw			248	49.2 (±1.1)

^{a} From signals of characteristic dad protons. ^{b} From signals of characteristic olefin protons.

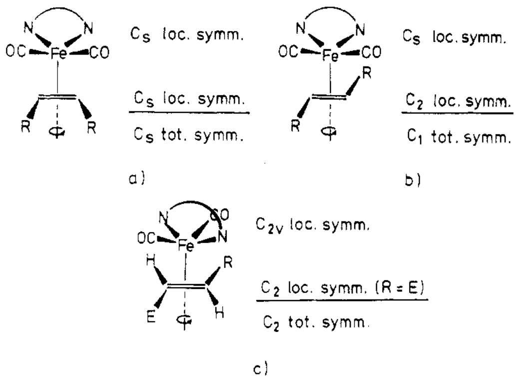

Figure 4. Symmetry considerations for olefin rotation in thermally exited square-pyramidal geometries of complexes **2**: (a) with cis-substituted olefins, e.g., **x** and **v**; (b) with trans-substituted olefins, e.g., **w** and **z**; (c) hypothetical higher exited geometry from which dad equilibration in **2aw** and **2dw** might be explained.

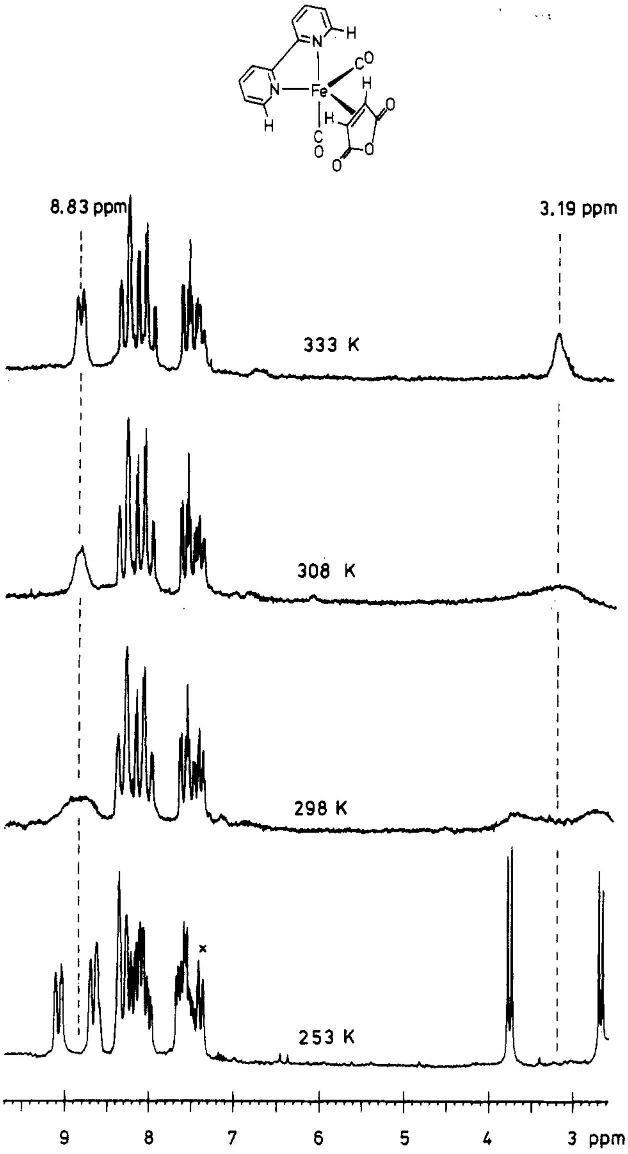

Figure 5. Structure of **2ay** corresponding to the rigid limiting situation at low temperature (253 K trace in Figure 5). The protons, the equilibration of which is demonstrated in Figure 5 (bpy-H(6,6′) centered at 8.83 ppm; maleic anhydride H centered at 3.19 ppm) are drawn out as H. ^{1}H NMR spectra of **2ay** (80 MHz; CD_3CN) at selected temperatures: a joint equilibration of the inequivalent dad and olefin halves, and hence a transition state of total C_s symmetry, can be deduced from the coalescence of the bipy-6,6′ and maleic anhydride protons at lowest and highest fields, respectively. For coalescence temperatures and calculated activation energies, cf. Table II. (x = impurity).

experience downfield coordination shifts of up to 1.2 ppm. Table I lists the chemical shifts for the olefinic protons in **2** and their respective coupling constants at the slow-exchange limit. The range of temperatures at which these limiting conditions are reached already indicates a pronounced influence of the respective ligand combinations on the exchange rates.

The molecular plane of an olefin upon coordination to an ML_n fragment loses its property as a plane of symmetry. The local symmetries of the olefin and of the ML_n fragment dictate the total symmetry of the complex, whereby only common symmetry elements are retained.

As mentioned above, in a trigonal-bipyramidal arrangement with dad and carbonyl ligands occupying the e/a and e′/a′ positions of Figure 3a, respectively, the total molecular symmetry is C_1 and the two halves of dad and olefin are inequivalent (as are the two CO ligands). With this in mind, we will investigate the mechanistic implications of Figure 3 for the ligand combinations in Table II. In other words, the symmetry properties of the intermediate square-pyramidal arrangement (Figure 3b) will be checked for compliance with the observed spectral changes upon raising the temperature from the slow-exchange limit.

(i) Olefins Derived from Maleic Acid (x, y). Figure 4a shows the local symmetries of the coordinated olefins **x** or **y** and of the (dad)Fe(CO)$_2$ fragment in the square-pyramidal geometry in which olefin rotation is supposedly taking place. The symmetry element C_s is common to both, and therefore the spectra of **2ax** and **2ay** in the limit of fast exchange should reflect the total C_s symmetry, which is actually the case (cf. Figure 5). Further, the inequivalent dad and olefin halves in the low-temperature spectra should equilibrate simultaneously. The numbers in Table II show that within the estimated margins of error,[16] the activation energies for dad and olefin equilibration at the temperatures of coalescence, $\Delta G_c^{\ddagger}$(dad) and $\Delta G_c^{\ddagger}$(ol), respectively, do agree fairly well.

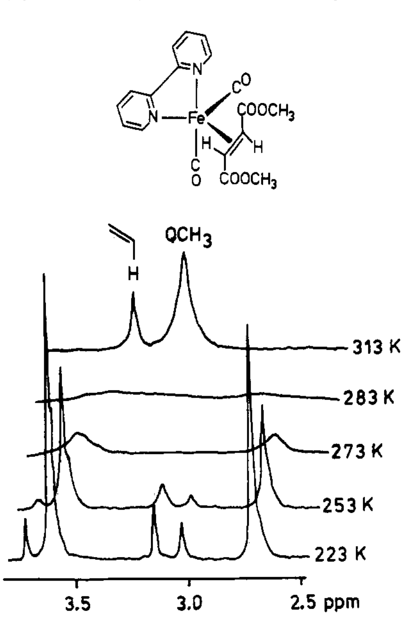

Figure 6. Structure of **2aw**. The mutually exchanging vinyl protons (AB part at 223 K) and methoxy protons in the olefin partial spectra in Figure 6 are drawn out as H. Partial ^1H NMR spectra of **2aw** (80 MHz; acetone-d_6) demonstrate the equilibration of the dimethyl fumarate resonances by means of rotation about the bond to iron which is coincident with the C_2 axis of the olefin.

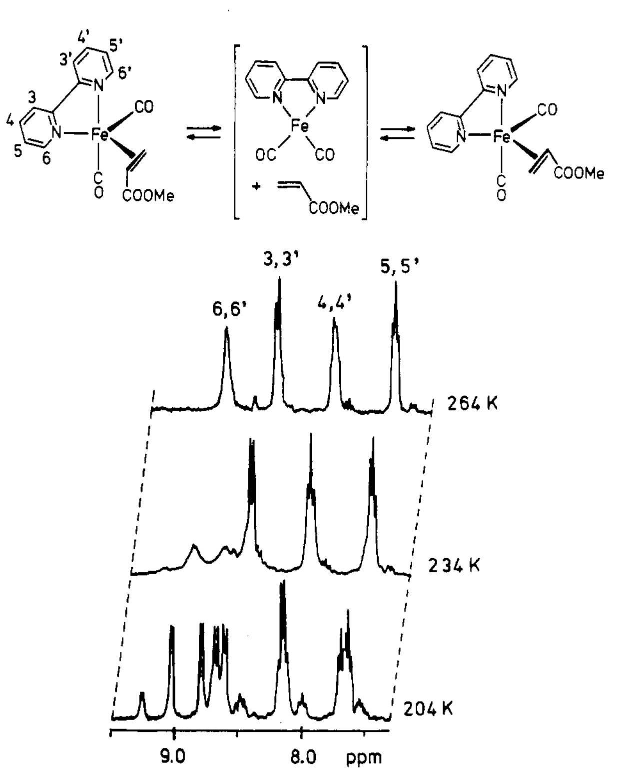

Figure 7. Structures of the two diastereomers of **2au** resulting from coordination of the methyl acrylate ligand via its *re* and *si* faces. It is not known which of the two represents the thermodynamically more stable species. Their interconversion and the equilibration of the bipyridyl halves are indicative of reversible olefin dissociation. Partial ^1H NMR spectra of **2au** (300 MHz; acetone-d_6) at selected temperatures showing (i) the equilibration of the two bipyridyl halves, which from symmetry considerations is not possible intramolecularly, and (ii) the disappearance of the minor diastereomer with increasing temperature.

(ii) Olefins Derived from Fumaric Acid (w, z). The total symmetry of the corresponding complexes **2aw**, **2dw**, **2ew**, **2fw**, and **2az** (cf. Table II) remains C_1 even in the transient square-pyramidal geometry (cf. Figure 4b) because the coordinated olefin (C_2) and the complex fragment (C_s) have no symmetry element in common. Fast performance of the C_2 operation on the olefin averages its two halves (cf. Figure 6), but the nuclei related by local C_s symmetry in the ligands of the ML_4 fragment should remain unisochronous. This behavior is found in all cases.

However, in the case of complexes **2aw** and **2dw**, both ^{13}C and ^1H NMR spectra indicate a second dynamic process at higher temperature, which is distinct from the former olefin rotation. The process is reversible with temperature and causes the equilibration of the two dad halves and the two carbonyl ligands. This equilibration might be rationalized by invoking an intermediate arrangement of total C_2 symmetry, e.g., an ML_4 fragment of C_{2v} symmetry as in Figure 4c, with the dad occupying two opposing basal positions. A vibrational distortion of the trigonal-bipyramidal ground-state geometry toward the arrangement in Figure 4c can be visualized; however, this would not conform with the usual bite angle N–Fe–N for a chelating dad of 80 ± 1°.[17] Thus, a dissociative process, as it is discussed below in the case of methyl acrylate, seems much more likely. Since the coalescence temperatures for this second process lie well above that for olefin equilibration, the thermal stability of the complexes becomes a limiting factor. With **2dw** the fast-exchange limit for the dad protons can be reached, but onset of decomposition gives rise to paramagnetic line broadening which, naturally, persists when cooling back to the slow-exchange limit. **2aw** decomposes even before complete coalescence is reached.

(iii) Methyl Acrylate. Methyl acrylate, representing a prochiral olefin, belongs to point group C_1 when coordinated to a metal. Therefore, regardless of its orientation and regardless of the local symmetry of the metal fragment, upon coordination it imposes total C_1 symmetry on the complex. In the acrylate complexes two diastereomeric forms are conceivable, and each of these may at low temperature possibly show stable rotamers. In the IR spectrum of a sample of complex **2au** that had been crystallized at low temperature, two additional, weaker carbonyl bands, appearing as shoulders on the main bands, indicated the presence of two isomers. The presence of two "real", i.e., nonrotameric diastereomers, resulting from coordination of the acrylate via its *re* and *si* faces, respectively, is confirmed by an extra set of proton resonances in the NMR spectrum (cf. the bpy part in Figure 7). In samples being crystallized, redissolved, and measured in the cold, a ratio of 3:1 was found for the integrals over the bpy signals of the two isomers. When the dissolved sample is warmed to room temperature, this ratio changes in favor of the major isomer, which, at 301 K, is the only species left. Regardless of the isomer, due to the lack of symmetry elements, the two dad halves should remain inequivalent, giving rise to two sets of resonances for the dad even in the transient geometries in Figure 3b or 4c. Nevertheless, this is only found at low temperatures (cf. Figure 7). On

---

(16) Sandström, J. *Dynamic NMR Spectroscopy*; Academic: New York, 1982.

(17) X-ray structures of the following iron complexes with chelating dad ligands of types A–C have been determined. Their geometries range from trigonal bipyramidal (**3a**) through intermediate (**3b**, **3e**) to square pyramidal with decreasing distortion in the given order of the latter three. The N–Fe–N angles are for (bipyridyl)tricarbonyliron (**3a**),[17a] 79.6°, for (2-benzoylpyridine anil)tricarbonyliron,[6] 79.4°, for [biacetyl bis(4-methoxyanil)]tricarbonyliron (**3e**),[17b] 79.4°, for (bipyridyl)(η^4-diethyl muconate)carbonyliron (**1av**),[5] 80.6°, for [glyoxal bis((2,6-diisopropylphenyl)imine)tricarbonyliron,[17c] 80.1°, and for (glyoxal bis(isopropylimine))(2,3-dimethylbuta-1,3-diene)carbonyliron,[3] 81.0°. (a) Frühauf, H.-W.; Krüger, C. "Proceedings of the XXI International Conference on Coordination Chemistry"; Toulouse, France, July 1980; Abstr. No. 36, unpublished. (b) Frühauf, H.-W.; Goddard, R. J., unpublished results. (c) Kokkes, M. W.; Stufkens, D. J.; Oskam, A. *J. Chem. Soc., Dalton Trans.* **1983**, 439.

warming, the double set of ^{1}H NMR resonances corresponding to the two inequivalent bipyridine halves of **2au** coalesces, and at 264 K a single set is observed. This is best interpreted by an intermediate reversible dissociation of the olefin whereby the local C_s symmetry of the (dad)-Fe(CO)$_2$ fragment determines the symmetry. The above-mentioned shift in the isomer ratio corroborates this explanation, as the two diastereomers again can only be interconverted by an intermediate decoordination of the olefin.

Correlating the observed NMR equilibration of the inequivalent dad halves with reversible olefin dissociation does imply that chemical exchange of the olefin ligands in complexes **2** should also be possible. This was indeed confirmed, as can be seen from the successful preparation of, e.g., **2ay** from **2au** (see Experimental Section). In a forthcoming paper[4] we will give a detailed account of the intimate dependence of substitutional lability on electronic donor/acceptor properties of the respective dad and olefin ligands in complexes **2**.

Kreiter et al.[18] have reported a phenomenologically related case, where complex fragments of local C_{2v} symmetry, [*mer*-(CO)$_3$W-*trans*-(PMe$_3$)$_2$], were coordinated to prochiral olefins and where the inequivalent PMe$_3$ signals were likewise found to equilibrate. The authors suggested that "fast rotation of the olefin ligand reduces the mutual symmetry interactions of olefin and complex fragment" and "the apparent change in symmetry, being a function of olefin rotation, causes the temperature dependence of the NMR signals of the complex ligands, e.g., of the two P ligands". Such reasoning has to be repudiated in principle. The symmetry properties of an entity cannot be subject to its frequency of rotation whatever this may be. A reinterpretation, e.g., in terms of a dissociative process, seems appropriate.

For the process of olefin rotation, the free energies of activation, listed in Table II, verify the dependence on the π-acidity of the olefin. But, before this is discussed in more detail, two points should be made clear. (i) In comparing these numbers, it has to be emphasized that they have been calculated from coalescence at various temperatures and not by complete line-shape analyses. They are therefore not corrected for temperature. (ii) It should be borne in mind that the activation energies $\Delta G_c^{\ddagger}$(ol) in Table II reflect the combined effects of the energetics for the tbp → sqp distortions (cf. Figure 3) and the actual olefin rotation. The latter should be particularly sensitive to electronic effects, i.e., variation in π-back-bonding, while the former would more obviously respond to steric effects. The following discussion illustrates both effects.

For the activation energies in complexes **2aw**, **2ax**, **2ay**, and **2az**, and as an overall trend, an increase in the direction of increasing acceptor properties of the olefins is evident. However, the small, or rather, negligible difference between the barriers in **2ax** and **2ay** is remarkable. The lower IR stretching frequencies for the carbonyl ligands in **2ax** [ν(CO) for **2ax** 1978.5 and 1912.5 cm^{-1} vs. 1987.0 and 1926.5 cm^{-1} for **2ay**] indicate stronger metal to carbonyl back-bonding than that in **2ay** and thus indicate that maleic anhydride (**y**) competes more effectively for electron density via back-bonding than does the dimethyl ester (**x**). Therefore the unexpectedly low barrier toward olefin rotation for the anhydride has to be ascribed to other than electronic, i.e., steric, reasons. The compact anhydride ring would certainly interfere less with the other ligands than fumarate with its two dangling ester groups.

Table III. Comparison of Activation Energies for Olefin Rotation in Fumarate Complexes 2 with Carbonyl Stretching Frequencies from Which Steric Hindrance by Biacetyl Bis(4-methoxyanil) (e) Is Inferred

complex	ν(CO), cm^{-1}	$\Delta G_c^{\ddagger}$(ol), kJ/mol
2fw	2004.0, 1951.0	49.2
2ew	1998.5, 1943.0	58.5
2dw	1991.5, 1937.5	52.9
2aw	1976.5, 1914.5	59.1

Just as the π-bond order between metal and olefin, and hence the barrier for olefin rotation, rises with rising π-acidity of the olefin, for a *given* olefin an increase in the effective donor strength of the dad ligand in **2** should have the same effect. The better donor is shifting more electron density toward the iron, and from there it is transmitted to the π-accepting olefin LUMO. In other words, from the free energies of activation for olefin rotation in **2** one should in principle be able to derive an order of relative donor strengths for the dad ligands also. However, such an order would also be subject to steric effects. In the series of fumarate complexes **2fw**, **2dw**, **2ew**, and **2aw** this is nicely demonstrated. Table III lists the activation energies for rotation of the fumarate ligand and compares them to the carbonyl stretching frequencies, as the latter constitute a second, independent measure for the electronic properties of the different dad ligands.

The good acceptor properties of the type C dad ligands, in particular those with *N*-aryl substituents, allow for less back-bonding to the other ligands, which is evidenced by the high CO stretching frequencies and by low $\Delta G_c^{\ddagger}$(ol) values. Only, the unexpectedly high $\Delta G_c^{\ddagger}$ value of **2ew** does not fit in this trend clearly. This has to be ascribed to steric hindrance inflicted by the dad ligand. Now, what is sterically so particular about the biacetyl bis(4-methoxyanil) moiety? It differs from its normally behaving, glyoxal-derived counterpart in **2fw** only by the methyl groups at the imine carbon atoms, and these are far away from the coordination center and point diametrically opposite to the other ligands. But, in the s-cis,anti,anti arrangement of the coordinated diazadiene, they interfere strongly with the nitrogen substituents,[19,20] and in this case, they force the aryl rings to be twisted out of the plane of the dad system. This presumably makes them an obstacle to the interligand angle deformations during the pseudorotation process and, maybe also, to the actual olefin rotation in the apical position of the intermediate square-pyramidal geometry.

Experimental Section

General Comments. All reactions were carried out under an atmosphere of argon. Technical grade solvents were purified and dried by standard techniques;[21] acetonitrile and tetrahydrofuran were pro analysis grade (E. Merck, Darmstadt). De-aeration was achieved by circular distillation under argon. The preparation of the starting (1,4-diaza-1,3-diene)tricarbonyliron complexes **3** has been described previously.[3,22] Olefins were technical or reagent grade and were distilled or sublimed prior to use. NMR spectra (^{1}H, ^{13}C) were obtained by using either a Bruker WP 80 SY WG, WH 270, or WM 300 spectrometer and are referenced to internal tetramethylsilane. Mass spectra (FI and FD mode, emitter 5 kV) were obtained from a Varian MAT 311 A and IR spectra from a Perkin-Elmer 283 spectrometer. Carbonyl

---

[18] Koemm, U.; Kreiter, C. G. *J. Organomet. Chem.* **1982**, *240*, 27.

[19] Bock, H.; tom Dieck, H. *Chem. Ber.* **1967**, *100*, 228.

[20] For further evidence on sterical crowding in tetrasubstituted diazabutadienes cf. Frühauf, H.-W.; Breuer, J. *J. Organomet. Chem.* **1986**, *301*, 183.

[21] Autorenkollektiv, *Organikum*; VEB Deutscher Verlag der Wissenschaften: Berlin, 1976.

[22] Frühauf, H.-W. *J. Chem. Res. Miniprint* **1983**, 2035.

stretching band positions were individually calibrated against appropriate rotational bands of deuterium chloride gas[23] and are accurate to within ±0.5 cm^{-1}. Elemental analyses were performed by the Microanalytical Laboratory Dornis and Kolbe, Mülheim a.d. Ruhr, Germany.

Preparation of (η^2-Diethyl muconate)(2,2′-bipyridyl)dicarbonyliron, 2av. At room temperature, a solution of ca. 500 mg (1.1 mmol) **1av**[3] in 100 mL of benzene was stirred under an atmosphere of CO until, after 2–3 days, a connected gas burette indicated an uptake of ca. 1.2 equiv of CO, and the originally reddish brown solution had acquired a deep green color. Then the residual amount of **1av**, which was less soluble than **2av**, was sufficiently low for the following workup. The solution was concentrated in vacuo beyond the point of beginning crystallization. *n*-Hexane (5–10 volumes) was added, and the violet solution of **3e** was inversely filtered off. The crystalline residue was repeatedly washed with hexane and recrystallized from toluene or acetone; yield ca. 320 mg (60%). Anal. Calcd for $C_{22}H_{22}FeN_2O_6$ (M_r 466.27): C, 56.67; H, 4.76; N, 6.01; Fe, 11.98. Found: C, 56.49; H, 4.88; N, 5.94; Fe, 11.84. IR (benzene) ν(CO) 1976.0, 1912.0 cm^{-1} ν(ester CO) 1692, 1592 cm^{-1}. ^{1}H NMR (270 MHz; acetone-d$_6$): T = 293 K (the bipy-resonances remain essentially unchanged in the observed temperature range from 233 to 318 K), δ 9.17/8.89 (H-6/6′, J(5,6) = 5.5 Hz), 8.48/8.38 (H-3/3′, J(3,4) = 8.0 Hz), 8.05/7.99 (H-4/4′, J(4,5) = 1.5 Hz, J(3,4) = 8.0 Hz) 7.61/7.59 (H-5/5′, J(4,5) = 1.5 Hz, J(5,6) = 5.5 Hz); muconate resonances with tentative assignments at three selected temperatures:

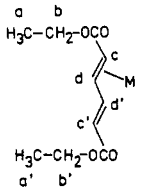

	δ		
	233 K	293 K	318 K
a′	1.08 (t, 3 H)	1.08 (t)	1.05 (t)
a	1.31 (t, 3 H)	1.12 (br)	1.10 (t)
c	3.17 (d, 1 H)	3.18 (d)	3.16 (d)
b, (+b′)	3.84 (m, 2 H)	3.87 (br)	3.81 (m, 4 H)
d, (+b′)	4.07 (m, 3 H)	4.04 (“t”)	4.02 (t, 1 H)
c′	4.74 (d, 1 H)	4.9 (br)	4.93 (d, br)
d′	5.03 (t, 1 H)	5.3 (br)	5.50 (br)

Preparation of (η^2-Diethyl muconate)[biacetyl bis(4-methoxyanil)]dicarbonyliron, 2ev. A solution of **1ev** was prepared by irradiating 0.76 g (1.74 mmol) of **3e** and 0.36 g (1.81 mmol) of diethyl muconate (v) in 130 mL of acetone for ca. 2 h with argon slowly bubbling through the solution. The solution was then syringed into a 250-mL flask that was continuously flushed with CO. After an additional 10 min of stirring under CO, the solvent was removed in vacuo and the residual **2ev** was recrystallized from acetone; yield 0.78 g (74%). IR (benzene): ν(CO) 1995.0, 1938.5 cm^{-1}, ν(ester CO) 1694, 1601 cm^{-1}. On standing in solution **2ev** may partially disproportionate to **1ev** and **3e**, as indicated by IR. ^{1}H NMR (80 MHz: acetone-d_6; ambient temperature; muconate resonances are tentatively assigned by the lettering given above for **2av**): δ 7.09 (s (br), 8 H, dad aryl H), 5.3–6.1 (m, 2 H, muco-c′/d′), 4.68 (“t”, 1 H, muco-d), 4.13 (q, 4 H, muco-b/b′, J = 7.8 Hz), 3.84 (s, 6H, dad-OCH$_3$), 2.92 (d, 1 H, muco-c, J = 10.0 Hz), 2.03 (ca. 6 H partially overlapping with solvent, dad-CH$_3$), 1.22/1.09 (t/t, 3 H/3 H, muco-a/a′, J = 7.6 Hz).

Photochemical Preparation of (η^2-Olefin)(1,4-diaza-1,3-diene)dicarbonyliron, 2. Photolyses were carried out in Pyrex glass (λ > 280 nm) immersion well reactors, using a high-pressure mercury arc (Philips HPK 125 W). At 12–15 °C, benzene solutions, ca. 1.5×10^{-2} M in starting tricarbonyliron complexes **3**, were irradiated in the presence of a given excess of the respective olefin with a continuous stream of argon bubbling through the solution. Reaction progress was monitored by IR, and, normally, irradiation was continued until no residual **3** was left. At room temperature in vacuo, the solutions were evaporated to dryness, and most of the excess olefin was condensed or sublimed to a cold finger containing liquid nitrogen. The residual raw product was redissolved, mostly in acetone, inversely filtered, and crystallized by cooling to −30 °C. For the individual complexes only deviations from this general procedure are given.

(η^2-Methyl acrylate)(2,2′-bipyridyl)dicarbonyliron, 2au: irradiation of 0.56 g (1.89 mmol) of **3a** with a tenfold molar excess of methyl acrylate for 3 h; crystallization from acetone/*n*-hexane (1:2 v/v) gave 0.58 g (87%) microcrystalline **2au**. IR and NMR spectra of this crop indicated a uniform product. Black-violet crystals obtained by recrystallization from pure acetone at −78 °C were identified as mixture of diastereomers (ca. 3:1), from which, on warming in solution, the major isomer was reproduced (see text). Anal. Calcd for $C_{16}H_{14}FeN_2O_4$ (M_r 354.15): C, 54.27; H, 3.98; N, 7.91. Found: C, 54.19; H, 4.03; N, 8.00. MS (EI): *m/e* 354 (M$^+$). IR (tetrahydrofuran): ν(CO) 1958.0, 1894.0 cm^{-1}; shoulders due to the minor diastereomer ca. 1963 and 1890 cm^{-1}. ^{1}H NMR (300 MHz; acetone-d_6): T = 204 K (limit of slow exchange), δ 8.67/8.60 (m/m, bpy-3,3′, ^3J(H,H) = 8.2 Hz), 8.16/8.13 (m/m, bpy-4,4′, ^3J(H,H) = 8.2 and 8.2 Hz), 7.69/7.63 (m/m, bpy-5,5′, ^3J(H,H) = 8.2 and 5.5 Hz), 9.02/8.78 (m/m, bpy-6,6′, ^3J(H,H) = 5.5 Hz), 3.23 (s, 3 H, OCH$_3$ acrylate); T = 264 K (limit of fast exchange), δ 8.51 (m, bpy-3,3′, ^3J(H,H) = 8.2 Hz), 8.05 (m, bpy-4,4′, ^3J(H,H) = 8.2 and 8.2 Hz), 7.58 (m, bpy-5,5′, ^3J(H,H) = 8.2 and 5.5 Hz), 8.90 (m, bpy-6,6′, ^3J(H,H) = 5.5 Hz), 3.28 (s, 3 H, OCH$_3$ acrylate).

(η^2-Dimethyl maleate)(2,2′-bipyridyl)dicarbonyliron, 2ax: irradiation of 0.69 g (2.33 mmol) of **3a** with fivefold molar excess in dimethyl maleate for 2 h. Two successive crystallizations from tetrahydrofuran and acetone gave 0.62 g (64%) of lustrous, black-violet **2ax**. Anal. Calcd for $C_{18}H_{16}FeN_2O_6$ (M_r 412.20): C, 52.45; H, 3.91; N, 6.80; Fe, 13.55. Found: C, 52.39; H, 3.92; N, 6.71; Fe, 13.62. MS (FI): *m/e* 412 (M$^+$). IR (tetrahydrofuran): ν(CO) 1978.5, 1912.5 cm^{-1}. ^{1}H NMR (80 Mz; CD$_3$CN): T = 253 K (limit of slow exchange), δ 8.36/8.26 (m/m, bpy-3,3′, ^3J(H,H) = 8.2 Hz), 8.05/7.98 (m/m, bpy-4,4′, ^3J(H,H) = 8.2 and 8.2 Hz), 7.55/7.46 (m/m, bpy-5,5′, ^3J(H,H) = 8.2 and 5.6 Hz), 9.05/8.60 (m/m, bpy-6,6′, ^3J(H,H) = 5.6 Hz), 3.00/1.55 (d/d, ═CH maleate, ^3J(H,H) = 9.1 Hz), 3.61/3.31 (s/s, OCH$_3$ maleate); T = 333 K (limit of fast exchange), δ 8.25 (m, bpy-3,3′, ^3J(H,H) = 8.2 Hz), 7.96 (m, bpy-4,4′, ^3J(H,H) = 8.2 and 8.2 Hz), 7.46 (m, bpy-5,5′, ^3J(H,H) = 8.2 and 5.6 Hz), 8.83 (m, bpy-6,6′, ^3J(H,H) = 5.6 Hz), 2.27 (br, ═CH maleate), 3.47 (s, OCH$_3$ maleate): ^{13}C NMR (20 MHz; CD$_3$CN): T = 328 K (limit of fast exchange), δ 218.4 (CO), 155.4 (bpy-2,2′), 123.5 (bpy-3,3′), 137.5 (bpy-4,4′), 126.4 (bpy-5,5′), 153.5 (bpy-6,6′), 49.4 (═CH maleate), 175.8 (carboxyl maleate), 51.0 (OCH$_3$ maleate).

(η^2-Dimethyl fumarate)(2,2′-bipyridyl)dicarbonyliron, 2aw: irradiation of 0.75 g (2.53 mmol) of **3a** with 0.73 g (5.06 mmol) of dimethyl fumarate for 2 h. After most of the excess fumarate was washed away with *n*-hexane, crystallization from acetone/*n*-hexane (10:1 v/v) yielded 0.80 g (77%) of red-violet **2aw**. Anal. Calcd for $C_{18}H_{16}FeN_2O_6$ (M_r 412.20): C, 52.45; H, 3.91; N, 6.80; Fe, 13.55. Found: C, 52.31; H, 3.89; N, 7.08; Fe, 13.93. MS (FI): *m/e* 412 (M$^+$). IR (tetrahydrofuran): ν(CO) 1976.5, 1914.5 cm^{-1}. ^{1}H NMR (80 MHz; acetone-d_6): T = 313 K (fast exchange only for fumarate), δ 8.50/8.37 (m/m, bpy-3,3′, ^3J(H,H) = 8.1 Hz), 8.08/8.00 (m/m, bpy-4,4′, ^3J(H,H) = 8.1 and 8.1 Hz), 7.60/7.57 (m/m, bpy-5,5′, ^3J(H,H) = 8.1 and 5.6 Hz), 9.20/8.75 (m/m, bpy-6,6′, ^3J(H,H) = 5.6 Hz), 3.40 (br, 2 H, ═CH fumarate), 3.17 (br, 6 H, OCH$_3$ fumarate); ^{13}C NMR (75.5 MHz; CD$_3$CN): T = 315 K (fast exchange only for fumarate; carboxylic carbons not observable due to coalescence), δ 218.9/216.9 (2 CO), 155.6/155.2 (quarternary bpy-2,2′), 123.5/122.8 (bpy-3,3′), 137.6/137.1 (bpy-4,4′), 126.2/125.9 (bpy-5,5′), 154.7/153.8 (bpy-6,6′), 50.8 (OCH$_3$ fumarate), 45.9 (═CH fumarate).

(η^2-Fumaronitrile)(2,2′-bipyridyl)dicarbonyliron, 2az: irradiation of 0.70 g (2.36 mmol) of **3a** with 0.60 g (7.69 mmol) of fumaronitrile in 150 mL of benzene for a total of 9 h whereafter 90% of **3a** had disappeared. The immersion well had to be cleaned intermediately from deposits. Residual **3a** was removed from the raw product by three consecutive 40-mL washings with *n*-hexane/benzene (3:1 v/v). The dried residue was redissolved in 10 mL acetone, and a total of 8 mL of n-hexane was added in portions

---

[23] Tables of Wavenumbers for the Calibration of Infrared Spectrometers, *Pure Appl. Chem.* **1960**, *1*, 537.

while the solution was stepwise cooled to −78 °C; yield 0.18 g (22%) of **2az** as beige-brown crystalline powder. Anal. Calcd for $C_{16}H_{10}FeN_4O_2$ (M_r 346.13): C, 55.52; H, 2.91; N, 16.19; Fe, 16.13. Found: C, 55.46; H, 3.15; N, 15.94; Fe, 16.21. MS (FD): *m/e* 346 (M^+). IR (tetrahydrofuran): ν(CO) 1988.0, 1929.5 cm^{-1}. ^{1}H NMR (80 MHz; CD_3CN): T = 293 K (limit of slow exchange), δ 8.42/8.31 (m/m, bpy-3,3′, ^3J(H,H) = 8.0 Hz), 8.07/8.00 (m/m, bpy-4,4′, ^3J(H,H) = 8.0 and 8.0 Hz), 7.56/7.47 (m/m, bpy-5,5′, ^3J(H,H) = 8.0 and 5.5 Hz), 9.16/8.58 (m/m, bpy-6,6′, ^3J(H,H) = 5.5 Hz), 2.73/2.27 (d/d, =CH fumaronitrile, ^3J(H,H) = 9.1 Hz).

(η^2-Dimethyl fumarate)(1,10-phenanthroline)dicarbonyliron, 2bw: irradiation of 0.25 g (0.78 mmol) of **3b** with 0.34 g (2.36 mmol) of fumarate for 45 min. After the usual workup 0.31 g (91%) of **2bw** was obtained in form of light red fine crystals. Due to their bad solubility they were not recrystallized but only washed with toluene and *n*-hexane, and then dried in vacuo. IR (tetrahydrofuran): ν(CO) 1977.0, 1915.0 cm^{-1}. ^{1}H NMR (80 MHz; acetone-d_6): T = 323 K (fast exchange appears to be reached only for the vinyl protons of the olefin): δ 8.66/8.58 (m/m, phen-4,7, ^3J(H,H) = 7.9 Hz), 7.98/7.94 (m/m, phen-3,8, ^3J(H,H) = 7.9 and 5.3 Hz), 9.55/9.07 (m/m, phen-2,9, ^3J(H,H) = 5.3 Hz), 8.12 (br, phen-5,6), 3.52 (br, =CH fumarate), 3.6/2.8 (br, OCH_3 fumarate).

(η^2-Dimethyl fumarate)(2-benzoylpyridine anil)dicarbonyliron, 2cw: irradiation of 0.90 g (2.26 mmol) of **3c** with ca. fivefold molar excess of fumarate for 1.5 h. During sublimation of the excess fumarate the flask exploded. Nevertheless, most of the raw product could be recovered, and after two successive recrystallizations from tetrahydrofuran/*n*-hexane (2:1 v/v) and toluene, respectively, 0.63 g (54%) of pure **2cw** was obtained in form of lustrous, brown-violet crystals. Anal. Calcd for $C_{26}H_{22}FeN_2O_6$ (M_r 514.33): C, 60.72; H, 4.31; N, 5.45. Found: C, 60.68; H, 4.30; N, 5.53. MS (FI): *m/e* 514 (M^+). IR (tetrahydrofuran): ν(CO) 1994.0, 1931.5 cm^{-1}. ^{1}H NMR (270 MHz; acetone-d_6): T = 303 K (limit of slow exchange), δ 8.84 (m, 1 H, py-6, ^3J(H,H) = 5.9 Hz), 7.59 (m, 1 H, py-3, ^3J(H,H) = 7.9 Hz), 7.91 (m, 1 H, py-4, ^3J(H,H) = 7.9 and 7.9 Hz), 7.58 (m, 1 H, py-5, ^3J(H,H) = 7.9 and 5.9 Hz), 7.0–7.5 (m, 10 H, phenyl), 4.01/3.35 (d/d, 1 H/1 H, =CH fumarate, ^3J(H,H) = 9.2 Hz), 3.60/2.81 (s/s, 3 H/3 H, OCH_3 fumarate).

(η^2-Dimethyl fumarate)(glyoxal bis(isopropylimine))dicarbonyliron, 2dw: irradiation of 0.43 g (1.54 mmol) of **3d** with 0.66 g (4.58 mmol) of fumarate for 2 h. Recrystallization from acetone/*n*-hexane (10:1 v/v) yielded 0.31 g (51%) of lustrous, black-violet crystals. Anal. Calcd for $C_{16}H_{24}FeN_2O_6$ (mw 396.24): C, 48.50; H, 6.11; N, 7.07; Fe, 14.09. Found: C, 48.60; H, 5.98; N, 6.99; Fe, 14.40. MS (FI): *m/e* 396 (M^+). IR (tetrahydrofuran): ν(CO) 1991.5, 1937.5 cm^{-1}. ^{1}H NMR (80 MHz; acetone-d_6): T 223 K (slow-exchange limit), δ 8.23/7.99 (s/s, =CH imine), 4.69/4.48 (sept/sept, =NCH(*i*-Pr), ^3J(H,H) = 6.5/6.8 Hz), 1.54/1.40 (d/d, —CH_3(*i*-Pr), ^3J(H,H) = 6.5/6.8 Hz), 4.05/3.13 (d/d, =CH fumarate, ^3J(H,H) = 9.9 Hz), 3.65/3.41 (s/s, OCH_3 fumarate); T = 313 K (fast-exchange limit for olefin; signs of coalescence also in the dad part), δ 8.1/7.8 (br/br, 1 H/1 H, =CH imine), 4.6 (br, 2 H, =NCH(*i*-Pr)), 1.5 (br, 12 H, CH_3 (*i*-Pr)), 3.65 (s, 2 H, =CH fumarate), 3.50 (s, 6 H, OCH_3 fumarate).

(η^2-Dimethyl fumarate)[biacetyl bis(4-methoxyanil)]dicarbonyliron, 2ew: irradiation of 0.62 g (1.42 mmol) of **3e** with ca. fivefold molar excess of fumarate for 1.75 h. Crystallization from acetone yielded 0.53 g (68%) of violet **2ew**. Anal. Calcd for $C_{26}H_{28}FeN_2O_8$ (M_r 552.37): C, 56.54; H, 5.11; N, 5.07. Found: C, 56.60; H, 5.14; N, 5.16. MS (FD): *m/e* 552 (M^+). IR (tetrahydrofuran): ν(CO) 1998.5, 1943.0 cm^{-1}. ^{1}H NMR (80 MHz; acetone-d_6): T = 223 K (limit of slow exchange), δ 2.20/1.96 (s/s, 3 H/3 H, CH_3 biacetyl), 3.88 (s, 6 H, OCH_3 anisyl), 6.8–7.8 (m, 8 H, aryl), 4.15/3.11 (d/d, 1 H/1 H, =CH fumarate, ^3J(H,H) = 10.5 Hz), 3.57/3.41 (s/s, 3 H/3 H, OCH_3 fumarate); T = 313 K (fast exchange for olefin only), δ 2.13/1.91 (s/s, 3 H/3 H, CH_3 biacetyl), 3.87 (s, 6 H, OCH_3 anisyl), 6.8–7.8 (m, 8 H, aryl), 3.67 (s, 2 H, =CH fumarate), 3.48 (s, 6 H, OCH_3 fumarate).

(η^2-Dimethyl fumarate)[glyoxalbis(4-methoxyanil)]dicarbonyliron, 2fw: irradiation of 0.78 g (1.91 mmol) of **3f** with 1.33 g (9.57 mmol) of fumarate. Though the photoreaction had been carried to completion, after the usual workup, and due to the pronounced lability of the metal–olefin bond, tricarbonyl **3f** was present again and had to be removed by washing with 10 mL of cold *n*-hexane. At 0 °C, the residue was redissolved in 50 mL of acetone, inversely filtered into a precooled flask, and stepwise cooled to −78 °C, yielding 0.67 g (67%) of fine black crystals. Anal. Calcd for $C_{24}H_{24}FeN_2O_8$ (M_r 524.33): C, 55.00; H, 4.61; N, 5.34. Found: C, 54.95; H, 4.58; N, 5.37. IR (tetrahydrofuran): ν(CO) 2004.0, 1951.0 cm^{-1}. ^{1}H NMR (80 MHz; acetone-d_6): T = 213 K (limit of slow exchange), δ 8.18/7.88 (d/d, 1 H/1 H, =CH imine, ^3J(H,H) = 0.5 Hz), 6.5–7.7 (m, 8 H, aryl), 3.85 (s, 6 H, OCH_3 anisyl), 4.18/2.96 (d/d, 1 H/1 H, =CH fumarate, ^3J(H,H) = 10.6 Hz), 3.83/3.73 (s/s, 3 H/3 H, OCH_3 fumarate).

Preparation of (η^2-Maleic anhydride)(2,2′-bipyridyl)dicarbonyliron, 2ay, via Thermal Substitution of Acrylate in 2au. To a solution of 0.12 g (0.34 mmol) **2au** in 5 mL tetrahydrofuran was added 0.17 g (1.73 mmol) of maleic anhydride. After 30 min at 30 °C the olefin exchange was completed (IR monitoring). Solvent and liberated acrylate were removed in vacuo, and the excess maleic anhydride was sublimed off, leaving 0.13 g (98%) of **2ay** which contained but traces of residual free anhydride as the sole impurity. MS (FD): *m/e* 366 (M^+). IR (tetrahydrofuran): ν(CO) 1987.0, 1926.5 cm^{-1}. ^{1}H NMR (80 MHz; acetone-d_6): T = 253 K (limit of slow exchange for all protons except, perhaps, bpy-3,3′ (cf. Figure 5); further cooling was not possible since the solution was already essentially depleted of complex, due to precipitation, necessitating excessive accumulation), δ 8.3 (d (br), 2 H, bpy-3,3′), 8.11/8.07 (m, bpy-4,4′, ^3J(H,H) = 7.8 and 7.3 Hz), 7.58/7.55 (m, bpy-5,5′, ^3J(H,H) = 7.3 and 5.6 Hz), 9.07/8.67 (m, bpy-6,6′, ^3J(H,H) = 5.6 Hz), 3.76/2.67 (d/d, =CH anhydride, ^3J(H,H) = 3.8 Hz); T = 333 K (limit of fast exchange not fully reached for bpy-6,6′ and anhydride protons), δ 8.30 (d, bpy-3,3′, ^3J(H,H) = 7.8 Hz), 8.05 (m, bpy-4,4′, ^3J(H,H) = 7.8 and 7.3 Hz), 7.53 (m, bpy-5,5′, ^3J(H,H) = 7.3 and 5.6 Hz), 8.83 (m (br), bpy-6,6′), 3.19 (s (br), =CH anhydride).

Acknowledgment. This work was supported by the Fonds der Chemischen Industrie.

Registry No. **1av**, 109007-87-6; **1dv**, 82134-03-0; **1ev**, 82134-11-0; **2au** (isomer 1), 108895-03-0; **2au** (isomer 2), 109007-88-7; **2av**, 108895-04-1; **2aw**, 108895-05-2; **2ax**, 109007-86-5; **2ay**, 108895-06-3; **2az**, 108895-07-4; **2bw**, 108895-08-5; **2cw**, 108895-09-6; **2dv**, 108895-12-1; **2dw**, 108895-10-9; **2ev**, 108918-83-8; **2ew**, 108895-11-0; **2fw**, 108918-84-9; **3a**, 82134-04-1; **3b**, 87882-37-9; **3c**, 74764-11-7; **3d**, 54446-62-7; **3e**, 65016-01-5; **3f**, 54446-64-9; u, 96-33-3; v, 6032-74-2; w, 624-49-7; x, 624-48-6; y, 108-31-6; z, 764-42-1.